IJCRT.ORG ISSN : 2320-2882

INTERNATIONAL JOURNAL OF CREATIVE RESEARCH THOUGHTS (IJCRT)

An International Open Access, Peer-reviewed, Refereed Journal

Role of Variable Liquid Properties on Oblique Stagnation Point Flow of a Casson Nanofluid with Convective Boundary Conditions

Jayashree D.N *.Prabhudeva N,

Department of Engineering Mathematics, Proudha Devaraya Institute of Technology, T.B. Dam, Hosapete, Karnataka, 583225, INDIA.

Abstract: Oblique stagnation point flow of a Casson nanofluid over a stretching surface is investigated under the influence of variable fluid properties. The effect of variable fluid properties on the flow field is examined by taking a convective boundary condition into account. Momentum, energy and concentration equations are transformed into the non-linear ODE system through suitable similarity transformations and are solved analytically via Semi numerical Technique (OHAM). Effect of pertinent parameters on dimensionless velocity, temperature and concentration are depicted graphically.

Keywords: Nanofluid; Stagnation point flow; Variable fluid properties; Convective heating.

Introduction:

The study of stagnation point flow has attained remarkable importance by numerous investigators due to their valuable manufacturing processes and industrial applications such as polymer extrusion, continuous casting of metals, wire drawing, glass blowing, etc. Two-dimensional stagnation point flow was first studied by Hiemenz [1]. Later, Matunobu [2-3] investigated the time-dependent flow structure and the wall shear stress near the stagnation point. Tamada [4] extended the work of Hiemenz [1] by considering two-dimensional stagnation point flow of a viscous fluid impinging on a plane stationary wall obliquely whereas Niimi et al. [5] solved the same for the axisymmetric case. Further, Chaim [6] investigated the effects of stagnation point flows (taking into account both two dimensional and axisymmetric flow) impinging both normally and obliquely on the stretching sheet. In view of this Mahapatra and Gupta [7] have studied two-dimensional orthogonal stagnation point flow over a stretching sheet. On the other hand, Nazar et al. [8], Reza and Gupta [9] extended the work of Mahapatra and Gupta [7] by considering unsteady flow and oblique stagnation point flow respectively. Wu et al. [10] examined the stagnation point flow in a porous medium. Labropulu et al. [11] investigated boundary layer nonorthogonal stagnation point flow of a viscoelastic second-grade fluid over a stretching surface considering the thermal boundary layer into account. Further, Makinde [12] examined the hydromagnetic mixed convection stagnation point flow with thermal radiation past a vertical plate embedded in a porous media. Several others have worked extensively on stagnation flows such as Makinde et al [13], Khan et al [14], Ibrahim and Makinde [15], Makinde et al [16] and Nadeem et al. [17].

In heat exchange forms, the convective boundary conditions assume a vital job, for instance in thermal combustion procedures, gas turbines, nuclear plants, and so forth. Convective boundary condition which is likewise called a Newton boundary condition is acquired from surface energy balance. Convective boundary condition corresponds to the existence of convection (heating/cooling) at the surface, which assumes that heat conduction at the surface of the material is equal to the heat convection at the surface in the same direction. In

perspective on this, numerous scientists have chipped away at convective boundary conditions [18– 21]. As of late, Ghaffari et al. [22] broadened the work of Labropulu et al. [11] by considering non-Newtonian nanofluid and convective boundary condition. Every one of these analysts has worked in the field of flow and heat transfer phenomena to be specific variable viscosity, variable thermal conductivity and variable diffusivity, which are essential for useful applications in innovative enterprises. The impact of these properties of the liquid can't be dismissed. Regardless, it is obvious from work by Prasad et al. [23] that the physical properties of the enveloping fluid may change with temperature, especially the fluid consistency and the fluid warm conductivity. For lubing up fluids, the heat created by the internal grinding and the relating climb in the temperature impacts the physical properties of the nanofluid, and the properties of the fluid are never again thought to be steady. The extension in temperature prompts a development in the vehicle ponders, in this way the heat trade at the divider is moreover affected. In this manner, to anticipate the flow and heat transfer rates, it is imperative to think about the variable liquid properties. Some increasingly significant writing is accessible in Refs. [24-28].

Motivated by the above research work, in the present paper, an investigation have been carried out to study the boundary layer oblique stagnation point flow of a Casson nanofluid in the presence of Newton boundary conditions. The convergence criteria of obtained solutions are built and exposed. The impact of important physical parameters such as liquid viscosity parameter, the Casson parameter, the constant ratio, the thermal conductivity parameter, variable species diffusivity parameter, the Prandtl number, thermophoresis parameter, the Brownian motion parameter, the Schmidt number and the Biot number on liquid velocity, temperature and concentration is examined graphically. The results are elaborated through graphs discussed their physical significance.

Formulation of the Problem:

A steady two-dimensional oblique flow of a viscous incompressible Casson nanofluid adjoining a stagnation point on a heated stretching sheet has been planned. The rheological equation of state for anisotropic and incompressible Casson fluid is given by (Ref. [29-30])

$$\tau_{ij} = \begin{cases} 2\left(\mu_B + P_y / \sqrt{2\pi}\right) e_{ij,} & \pi > \pi_c \\ 2\left(\mu_B + P_y / \sqrt{2\pi_c}\right) e_{ij,} & \pi < \pi_c \end{cases}$$

where $\pi = e_{ij} e_{ij}$ and e_{ij} is the $(i, j)^{\text{th}}$ component of deformation rate, π is the product of component with itself, π_c is a critical value of this product based on the non-Newtonian model, μ_B is the plastic dynamic viscosity of the non-Newtonian fluid and P_y is the yield stress of the fluid. Let the heated surface be along $\bar{y} = 0$, the origin O is fixed at the stagnation point. Assume that the flow is confined to $\bar{y} > 0$. Two equal and opposite forces are applied along $\bar{x}$-axis so as to stretch the sheet keeping the origin O fixed. Further, it is anticipated that the stretching sheet has linear velocity $U_w = c\bar{x}$ and temperature $T_w > T_\infty$, where T_∞ is the uniform temperature of the ambient fluid.

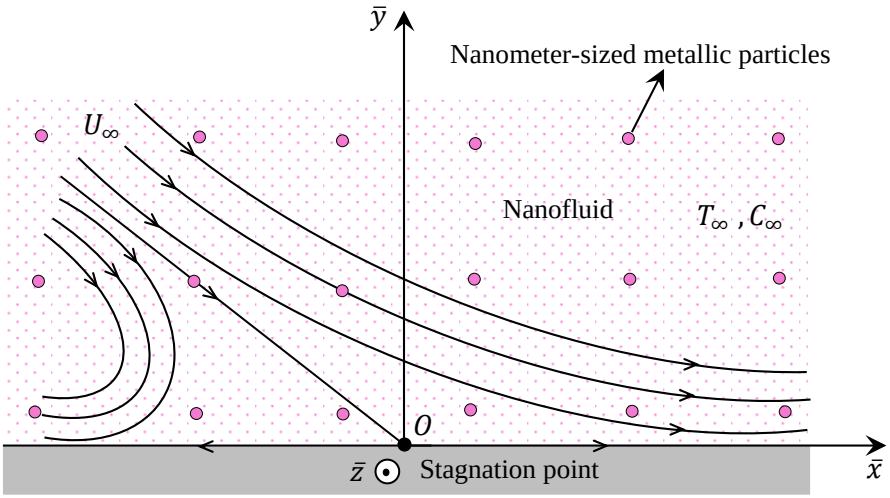

Fig. 1: Physical model of the problem

In view of these assumptions, the governing equations for oblique stagnation point flow over a linearly stretching sheet with varying fluid properties (variation of fluid viscosity and fluid thermal conductivity with temperature) are written as

$$\frac{\partial \bar{u}}{\partial \bar{x}} + \frac{\partial \bar{v}}{\partial \bar{y}} = 0, \tag{1}$$

$$\left\{\bar{u}\frac{\partial \bar{u}}{\partial \bar{x}} + \bar{v}\frac{\partial \bar{u}}{\partial \bar{y}} + \frac{1}{\rho_\infty}\frac{\partial \bar{p}}{\partial \bar{x}}\right\} = \left(1+\frac{1}{\beta}\right)\frac{1}{\rho_\infty}\bar{\nabla}\left(\mu(\bar{T})\bar{\nabla}\bar{u}\right), \tag{2}$$

$$\left\{\bar{u}\frac{\partial \bar{v}}{\partial \bar{x}} + \bar{v}\frac{\partial \bar{v}}{\partial \bar{y}} + \frac{1}{\rho_\infty}\frac{\partial \bar{p}}{\partial \bar{y}}\right\} = \left(1+\frac{1}{\beta}\right)\frac{1}{\rho_\infty}\bar{\nabla}\left(\mu(\bar{T})\bar{\nabla}\bar{v}\right), \tag{3}$$

$$\bar{u}\frac{\partial \bar{T}}{\partial \bar{x}} + \bar{v}\frac{\partial \bar{T}}{\partial \bar{y}} = \frac{\partial}{\partial \bar{x}}\left(\alpha(\bar{T})\frac{\partial \bar{T}}{\partial \bar{x}}\right) + \frac{\partial}{\partial \bar{y}}\left(\alpha(\bar{T})\frac{\partial \bar{T}}{\partial \bar{y}}\right) + \frac{(\rho C)_p}{(\rho C)_\infty}\left[D_B(\bar{C})\bar{\nabla}\bar{C}.\bar{\nabla}\bar{T} + \frac{D_T}{T_\infty}\bar{\nabla}\bar{T}.\bar{\nabla}\bar{T}\right], \tag{4}$$

$$\bar{u}\frac{\partial \bar{C}}{\partial \bar{x}} + \bar{v}\frac{\partial \bar{C}}{\partial \bar{y}} = \frac{\partial}{\partial \bar{x}}\left(D_B(\bar{C})\frac{\partial \bar{C}}{\partial \bar{x}}\right) + \frac{\partial}{\partial \bar{y}}\left(D_B(\bar{C})\frac{\partial \bar{C}}{\partial \bar{y}}\right) + \frac{D_T}{T_\infty}\bar{\nabla}^2\bar{T}. \tag{5}$$

These partial differential equations (PDEs) are subjected to the following boundary conditions

$$\begin{aligned} &\bar{u} = c\bar{x} \;,\; \bar{v} = 0 \;,\; -\alpha_\infty \frac{\partial \bar{T}}{\partial \bar{y}} = \lambda\left(T_f - \bar{T}\right) \;,\; \bar{C} = C_w \quad \text{at} \quad \bar{y} = 0, \\ &\bar{u} = a\bar{x} + b\bar{y} \;,\; \bar{T} = T_\infty \;,\; \bar{C} = C_\infty \quad \text{as} \quad y \to \infty. \end{aligned} \tag{6}$$

Here, $\bar{u}$ and $\bar{v}$ are the velocity components along $\bar{x}$ and $\bar{y}$ directions, ρ_∞ and ρ_p are the constant fluid density and nanoparticles density, respectively, β is the Casson parameter, $\bar{p}$ is the pressure of the fluid, $\bar{T}$ and $\bar{C}$ are the temperature and concentration of the fluid, respectively, whereas T_∞ and C_∞ represent their ambient values, σ is the fluid electrical conductivity, $\mu(\bar{T})$ is the temperature dependent viscosity , $\alpha(\bar{T})$ is the temperature dependent thermal diffusivity and $D_B(\bar{C})$ is the species diffusivity. In this investigation, the physical quantities $\mu(\bar{T})$, $\alpha(\bar{T})$ and $D_B(\bar{C})$ are taken in the following form

$$\frac{1}{\mu(\bar{T})}=\frac{1}{\mu_\infty}\left[1+\delta\left(\bar{T}-T_\infty\right)\right], \tag{7}$$

$$\alpha(\bar{T})=\alpha_\infty\left[1+\varepsilon_1\left(\frac{\bar{T}-T_\infty}{T_f-T_\infty}\right)\right], \tag{8}$$

$$D_B(\bar{C})=D_\infty\left[1+\varepsilon_2\left(\frac{\bar{C}-C_\infty}{C_w-C_\infty}\right)\right], \tag{9}$$

where μ_∞, α_∞ and D_∞ are the ambient fluid viscosity, the thermal conductivity and the species diffusivity, respectively, ε_1 and ε_2 are small parameters known as the variable thermal diffusivity and the variable species diffusion parameters, (a,b,c) are positive constants with dimensions of inverse time and λ is the convective heat transfer coefficient. After introducing the following quantities

$$x=\bar{x}\sqrt{\frac{c}{\nu_\infty}},\ y=\bar{y}\sqrt{\frac{c}{\nu_\infty}},\ u=\frac{1}{\sqrt{\nu_\infty c}}\bar{u},\ \mathrm{v}=\frac{1}{\sqrt{\nu_\infty c}}\bar{\mathrm{v}},\ p=\frac{1}{\mu_\infty c}\bar{p},\ T=\frac{\bar{T}-T_\infty}{T_f-T_\infty},\ C=\frac{\bar{C}-C_\infty}{C_w-C_\infty}, \tag{10}$$

Eqs. (1) - (6) become

$$\frac{\partial u}{\partial x}+\frac{\partial \mathrm{v}}{\partial y}=0, \tag{11}$$

$$u\frac{\partial u}{\partial x}+\mathrm{v}\frac{\partial u}{\partial y}+\frac{1}{\rho_\infty}\frac{\partial p}{\partial x}=\left(1+\frac{1}{\beta}\right)\frac{1}{\rho_\infty}\frac{\partial}{\partial x}\left[\frac{1}{(1-T/\theta_r)}\frac{\partial u}{\partial x}\right]+\frac{1}{\rho_\infty}\left(1+\frac{1}{\beta}\right)\frac{\partial}{\partial y}\left[\frac{1}{(1-T/\theta_r)}\frac{\partial u}{\partial y}\right], \tag{12}$$

$$u\frac{\partial \mathrm{v}}{\partial x}+\mathrm{v}\frac{\partial \mathrm{v}}{\partial y}+\frac{1}{\rho_\infty}\frac{\partial p}{\partial y}=\frac{1}{\rho_\infty}\left(1+\frac{1}{\beta}\right)\frac{\partial}{\partial y}\left[\frac{1}{(1-T/\theta_r)}\frac{\partial \mathrm{v}}{\partial y}\right]+\left(1+\frac{1}{\beta}\right)\frac{1}{\rho_\infty}\frac{\partial}{\partial x}\left[\frac{1}{(1-T/\theta_r)}\frac{\partial \mathrm{v}}{\partial x}\right], \tag{13}$$

$$\mathrm{Pr}\left(u\frac{\partial T}{\partial x}+\mathrm{v}\frac{\partial T}{\partial y}\right)=\frac{\partial}{\partial x}\left[(1+\varepsilon_1 T)\frac{\partial T}{\partial x}\right]+\frac{\partial}{\partial y}\left[(1+\varepsilon_1 T)\frac{\partial T}{\partial y}\right]+\mathrm{Pr}\left[\begin{matrix}Nb\,(1+\varepsilon_2 C)\nabla C.\nabla T\\+Nt\,\nabla T.\nabla T\end{matrix}\right], \tag{14}$$

$$Sc\left(u\frac{\partial C}{\partial x}+\mathrm{v}\frac{\partial C}{\partial y}\right)=\frac{\partial}{\partial x}\left[(1+\varepsilon_2 C)\frac{\partial C}{\partial x}\right]+\frac{\partial}{\partial y}\left[(1+\varepsilon_2 C)\frac{\partial C}{\partial y}\right]+\frac{Nt}{Nb}\nabla^2 T, \tag{15}$$

Here, $\theta_r=(T_r-T_\infty)/(T_f-T_\infty)$ and $T_r=T_\infty-\delta^{-1}$. (16)

By making use of the stream function formulation $\left(\text{i.e., } (u,\mathrm{v})=(\partial\psi/\partial y,-\partial\psi/\partial x)\right)$ and seeking analytical solutions of the form $\psi(x,y)=xf(y)+g(y)$, $T=\theta(y)$ and $C=\phi(y)$, we obtain

$$\left(1+\frac{1}{\beta}\right)\left(\frac{f''}{1-\theta/\theta_r}\right)'+ff''-f'^2+C_1=0, \tag{17}$$

$$\left(1+\frac{1}{\beta}\right)\left(\frac{g''}{1-\theta/\theta_r}\right)'+fg''-f'g'+C_2=0, \tag{18}$$

$$\left[(1+\varepsilon_1\theta)\theta'\right]'+\mathrm{Pr}\,f\,\theta'+\mathrm{Pr}\,Nb\,(1+\varepsilon_2\phi)\phi'\theta'+\mathrm{Pr}\,Nt\,\theta'^2=0, \tag{19}$$

$$\left[(1+\varepsilon_2\phi)\phi'\right]'+Sc\,f\,\phi'+\frac{Nt}{Nb}\theta''=0, \tag{20}$$

$$\begin{aligned}&f(0)=0,\ f'(0)=1,\ g(0)=0,\ g'(0)=0,\theta'(0)=-\gamma(1-\theta(0)),\phi(0)=1\\&f'(\infty)=\frac{a}{c},\ g''(\infty)=\gamma_1,\ \theta(\infty)=0,\ \phi(\infty)=0,\end{aligned} \tag{21}$$

It worth mentioning here that the functions $f(y)$ and $g(y)$ used above are referring to normal and tangential components of the nanofluid flow, whereas C_1 and C_2 are their corresponding integration constants. Moreover, the physical parameters Prandtl number (Pr), Thermophoresis parameter (Nt), Brownian motion parameter (

Nb), Biot number (Bi), and Schmidt number (Sc) are shown in Eqs. (17), (19), (20) and (21) are expressed as follows

$$\Pr=\frac{\nu_\infty}{\alpha_\infty}, Nt=\frac{D_T}{T_\infty}\frac{(\rho C)_p}{(\rho C)_f}\frac{(T_f-T_\infty)}{\nu_\infty}, Nb=D_\infty\frac{(\rho C)_p}{(\rho C)_f}\frac{(C_w-C_\infty)}{\nu_\infty}, \gamma=\frac{h}{\alpha_\infty}\sqrt{\frac{\nu_\infty}{c}}, Sc=\frac{\nu_\infty}{D_\infty}. \quad (22)$$

Invoking the boundary conditions $f'(\infty)=a/c$ and $g''(\infty)=\gamma_1$ in Eqs. (17) and (18), we obtain

$$C_1=\frac{a^2}{c^2}, \quad (23)$$

$$f(y)=\left(\frac{a}{c}\right)y+A \quad \text{at} \quad y\to\infty, \quad (24)$$

$$C_2=-A\gamma_1. \quad (25)$$

where, A is a constant, whose value depends on a/c, θ_r, ε_1, ε_2, $\Pr$, Nb and Nt. Let us introduce the new function $g'(y)=\gamma_1 h(y)$ in Eq. (18) to get

$$\left(1+\frac{1}{\beta}\right)\left(\frac{h'}{1-\theta/\theta_r}\right)'+fh'-hf'-A=0. \quad (26)$$

The quantities of physical interest are respectively the Skin friction coefficient C_{fx}, the Nusselt number Nu_x and the Sherwood number Sh_x, which are defined as

$$C_{fx}=\frac{2\tau_w}{\rho_\infty U_w^2}, Nu_x=\frac{\bar{x}q_w}{k_\infty(T_f-T_\infty)}, Sh_x=\frac{\bar{x}q_m}{\rho_p D_\infty(C_w-C_\infty)}, \quad (27)$$

where $\tau_w=\mu(\bar{T})\left.\frac{\partial\bar{u}}{\partial\bar{y}}\right|_{\bar{y}=0}+\mu(\bar{T})\left.\frac{\partial\bar{v}}{\partial\bar{x}}\right|_{\bar{y}=0}, q_w=-k(\bar{T})\left.\frac{\partial\bar{T}}{\partial\bar{y}}\right|_{\bar{y}=0}, q_m=-\rho_p D_B(\bar{C})\frac{\partial\bar{C}}{\partial\bar{y}}.$ (28)

In dimensionless form these quantities become

$$C_{fx}=\frac{2(xf''(0)+\gamma_1 h'(0))}{(1-\theta(0)/\theta_r)x^2}, \quad (29)$$

$$\mathrm{Re}_x^{-1/2}Nu_x=-(1+\varepsilon_1\theta(0))\theta'(0), \quad (30)$$

$$\mathrm{Re}_x^{-1/2}Sh_x=-(1+\varepsilon_2)\phi'(0), \quad (31)$$

Here, Re_x is the local Reynolds number, where $\mathrm{Re}_x=U_w\bar{x}/\nu_\infty$.

Semi-analytical solution:

Optimal homotopy analysis method has been employed to solve the following nonlinear system of ODEs (For more details see Liao [31] and Van Gorder [32])

$$\left(1+\frac{1}{\beta}\right)\left(\frac{f''}{1-\theta/\theta_r}\right)'+ff''-f'^2+\frac{a^2}{c^2}=0,$$

$$\left(1+\frac{1}{\beta}\right)\left(\frac{h'}{1-\theta/\theta_r}\right)'+fh'-hf'-A=0, \quad (32)$$

$$\left[(1+\varepsilon_1\theta)\theta'\right]'+\Pr f\theta'+\Pr Nb(1+\varepsilon_2\phi)\phi'\theta'+\Pr Nt\theta'^2=0,$$

$$\left[(1+\varepsilon_2\phi)\phi'\right]'+Sc\, f\phi'+\frac{Nt}{Nb}\theta''=0,$$

with their appropriate boundary conditions boundary conditions

$$f(y)=0 \;,\; f'(y)=1 \;,\; h(y)=0 \;,\; \theta'(y)=-\gamma\left(1-\theta(y)\right) \;,\; \phi(y)=1 \quad \text{at} \quad y=0,$$
$$f'(y)=\frac{a}{c} \;,\; h'(y)=1 \;,\; \theta(y)=0 \;,\; \phi(y)=0 \quad \text{as} \quad y\to\infty. \tag{33}$$

In accordance with the above boundary conditions, we assume the initial guess and linear operator as

$$f(y)=\frac{a}{c}y+\left(1-\frac{a}{c}\right)\left(1-e^{-y}\right) \;,\; h(y)=y \;,\; \theta(y)=\frac{\gamma}{\gamma+1}e^{-y} \;,\; \phi(y)=e^{-y} \;, \tag{34}$$

$$L_f=\frac{d^3f}{dy^3}-\frac{df}{dy} \;,\; L_h=\frac{d^2h}{dy^2}-h \;, L_\theta=\frac{d^2\theta}{dy^2}-\theta \;,\; L_\phi=\frac{d^2\phi}{dy^2}-\phi \;. \tag{35}$$

Here, the linear operators L_f , L_h , L_θ and L_ϕ verify the following properties

$$L_f\left(c_1+c_2e^{y}+c_3e^{-y}\right)=0 \;,\; L_h\left(c_4+c_5e^{-y}\right)=0 \;, L_\theta\left(c_6+c_7e^{-y}\right)=0 \;,\; L_\phi\left(c_8+c_9e^{-y}\right)=0 \;. \tag{36}$$

Here, c_i are arbitrary constants, where $1\le i\le 9$. By introducing the following expressions

$$f(y)=\sum_{m=1}^{\infty}f_m q^m \;,\; h(y)=\sum_{m=1}^{\infty}h_m q^m \;, \theta(y)=\sum_{m=1}^{\infty}\theta_m q^m \;,\; \phi(y)=\sum_{m=1}^{\infty}\phi_m q^m \;, \tag{37}$$

the m^{th} order deformation equations are obtained as

$$L_f\left[f_m(y)-\chi_m f_{m-1}(y)\right]=\hbar_f R_m^{\,f}(y) \;,\; L_h\left[h_m(y)-\chi_m h_{m-1}(y)\right]=\hbar_h R_m^{\,h}(y) \;,$$
$$L_\theta\left[\theta_m(y)-\chi_m\theta_{m-1}(y)\right]=\hbar_\theta R_m^{\,\theta}(y) \;,\; L_\phi\left[\phi_m(y)-\chi_m\phi_{m-1}(y)\right]=\hbar_\phi R_m^{\,\phi}(y) \;, \tag{38}$$

in which

$$f_m(0)=0 \;,\; f_m'(0)=0 \;, h_m(0)=0, \theta_m'(0)-\gamma\theta_m(0)=0 \;, \phi_m(0)=0.$$
$$f_m'(\infty)=0 \;,\; h_m'(\infty)=0 \;, \theta_m(\infty)=0 \;,\; \phi_m(\infty)=0 \;. \tag{39}$$

In addition, the residual terms $R_m^{\,f}(y)$, $R_m^{\,h}(y)$, $R_m^{\,\theta}(y)$ and $R_m^{\,\phi}(y)$ are obtained by substituting the expressions of Eq. (37) in the set of differential equations described above by Eq. (32), where

$$\chi_m=\begin{cases}0 & \text{if} \quad m\le 1,\\ 1 & \text{if} \quad m>1.\end{cases} \tag{40}$$

Now we evaluate the error and minimize over $\hbar_f,\hbar_h,\hbar_\theta,\hbar_\phi$ in order to obtain the optimal values of $\hbar_f,\hbar_h,\hbar_\theta,\hbar_\phi$ and least possible error. At m^{th} order deformation equation, the exact residual errors are given by

$$E_m^{\,f}(\hbar_f)=\frac{1}{(M+1)}\sum_{k=0}^{M}\left[N_f\left(\sum_{n=0}^{m}f_n(y_k)\right)\right]^2 \;,\; E_m^{\,h}(\hbar_h)=\frac{1}{(M+1)}\sum_{k=0}^{M}\left[N_h\left(\sum_{n=0}^{m}h_n(y_k)\right)\right]^2 \;,$$
$$E_m^{\,\theta}(\hbar_\theta)=\frac{1}{(M+1)}\sum_{k=0}^{M}\left[N_\theta\left(\sum_{n=0}^{m}\theta_n(y_k)\right)\right]^2 \;,\; E_m^{\,\phi}(\hbar_\phi)=\frac{1}{(M+1)}\sum_{k=0}^{M}\left[N_\phi\left(\sum_{n=0}^{m}\phi_n(y_k)\right)\right]^2 . \tag{41}$$

Moreover, it is worth noting here that $E_m^{\,f}(\hbar_f)$, $E_m^{\,h}(\hbar_h)$, $E_m^{\,\theta}(\hbar_\theta)$ and $E_m^{\,\phi}(\hbar_\phi)$ are minimized to get the optimal values of $\hbar_f$, $\hbar_h$, $\hbar_\theta$ and $\hbar_\phi$, where $y_k=k/M$ and $0\le k\le M$.

Results and Discussion

The parameters affecting the stagnation point fluid flow, heat and mass transfer are fluid viscosity parameter θ_r, the Casson parameter β the constant a/c, the thermal conductivity parameter ε_1, variable species diffusivity parameter ε_2, the Prandtl number Pr, thermophoresis parameter Nt, the Brownian motion parameter Nb, the Schmidt number Sc and the Biot number γ. Results are presented through graphs (Figs. 3-

8). It is seen that the profiles of $f'(y)$, $h'(y)$, $\theta(y)$ and $\phi(y)$ tends asymptotically to zero. The impact of a/c on $f'(y)$, $h'(y)$, $\theta(y)$ and $\phi(y)$ is depicted in Fig. 3(a-d).

It is clear from Fig. 3(a) that $f'(y)$ increases for increasing values of a/c . For $a/c > 1$ the flow has boundary layer structure and thickness of this boundary layer decreases for increasing values of a/c . This is due to the fact that for a fixed value of c, as a increases, the strain at the stagnation point also increases, which in turn accelerates the free stream and hence the boundary layer thickness decreases. Moreover, $a/c < 1$ implies that stretching velocity cx of the sheet surpasses the stagnation velocity ax. Hence, the flow has an inverted boundary layer structure.

Fig 3(b) portrays the influence of a/c on $h'(y)$, for $a/c < 1$, the profile of $h'(y)$ initially increases for increasing values of a/c later at a certain point after $y = 1$ the flow gets reversed. Exactly the opposite trend is observed when $a/c > 1$. From Fig 3(c-d), it is clear that both temperature and concentration profiles decline with the rise in a/c . Fig. 4(a-d) shows the impact of θ_r and β on $f'(y)$, $h'(y)$, $\theta(y)$ and $\phi(y)$. It is obvious from Fig. 4(a) that the profile of $f'(\xi)$ decreases for larger values of θ_r. This is credited to the fact that the fluid viscosity depends inversely on the temperature difference between the wall and the ambient fluid. So, there is a collapse in the momentum boundary layer thickness. On the other hand, the reverse impression is observed on temperature and concentration boundary layer thicknesses (see Fig. 4(c-d)). There is a dual effect of θ_r on $h'(y)$ (recorded in Fig. 4(b)), the transverse velocity increases near the plate and as one moves away from the plate the velocity decreases. The effect of β is to decrease the momentum boundary layer thickness and is due to the fact that as Casson parameter approaches larger values, fluid behaves like a Newtonian fluid. Physically, an increase in β means $(as \beta \to \infty)$, a decrease in the yield stress is recorded and hence decreasing pattern of velocity profiles is seen, whereas the reverse trend is observed in case of temperature and concentration profiles (see Fig. 4(a-d)).

The impact of Brownian motion parameter Nb and the Thermophoresis parameter on the temperature and concentration profiles are depicted in Fig 5(a-b). With the increase of values of Nb, more and more heat is transferred and hence there is an enhancement in the thermal boundary layer thickness and in turn temperature profile upsurges. On the other hand, the reverse phenomenon is seen for the concentration profile. Thermophoresis force gets enhanced with Nt, which results in the augmentation of concentration boundary layer thickness and concentration profile. In this case, the nanoparticles move away from the hot sheet towards the ambient fluid. Hence, the same trend is observed in both the profiles, namely temperature as well as concentration. (see Fig 5(a-b)).

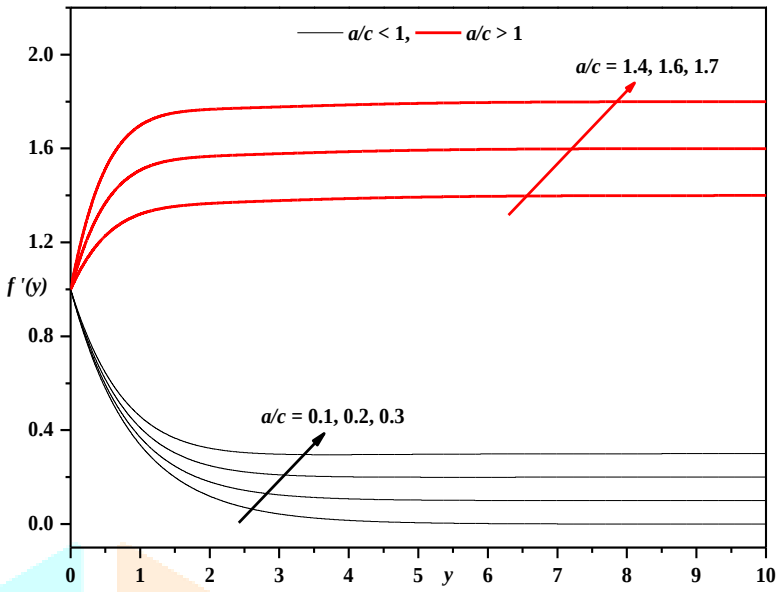

Fig.3(a):Axial velocity profile for different values of *a/c* with *Pr* = 1, *Sc* = 1, *Nt* = 0.1, *Nb* = 0.1, ε_1 = 0.1, ε_2 = 0.1, θ_r = -5, β = 2, γ = 0.5.

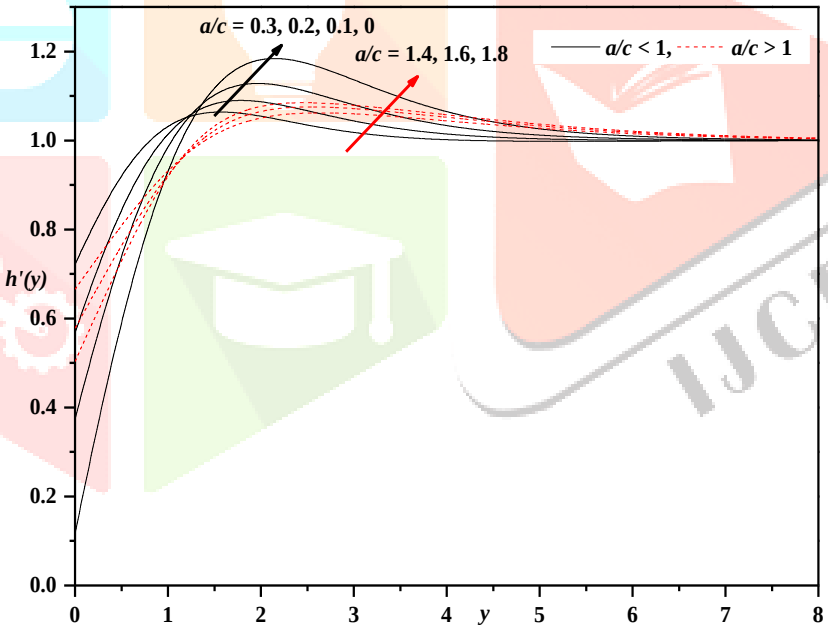

Fig.3(b):Transverse velocity profile for different values of *a/c* with *Pr* = 1, *Sc* = 1, *Nt* = 0.1, *Nb* = 0.1, ε_1 = 0.1, ε_2 = 0.1, θ_r = -5, β = 2, γ = 0.5.

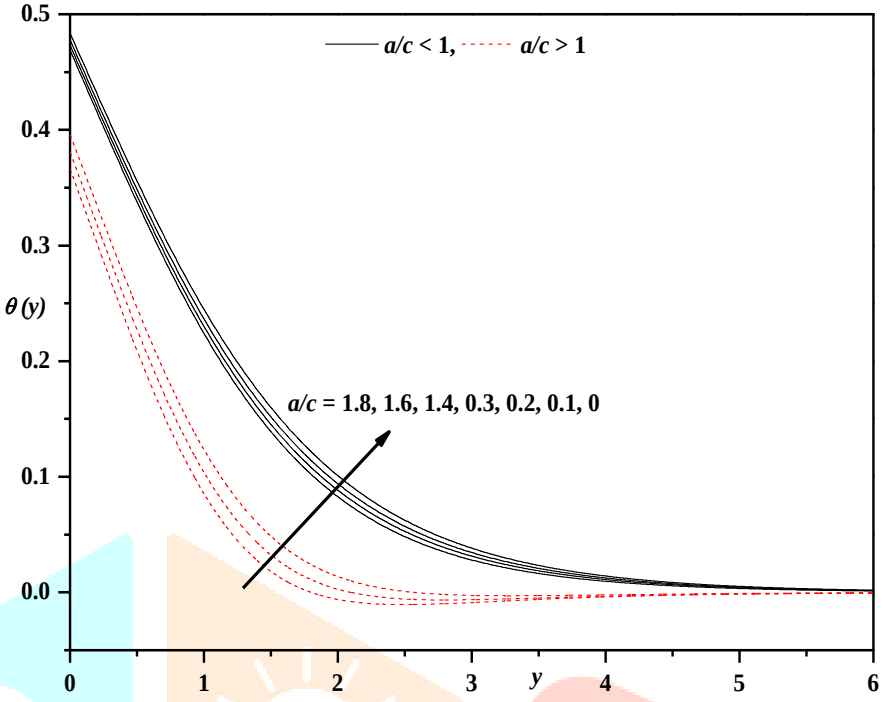

Fig.3(c):Temperature profile for different values of *a/c* with *Pr* = 1, *Sc* = 1, *Nt* = 0.1, *Nb* = 0.1, ε_1 = 0.1, ε_2 = 0.1, θ_r = -5, β = 2, γ = 0.5.

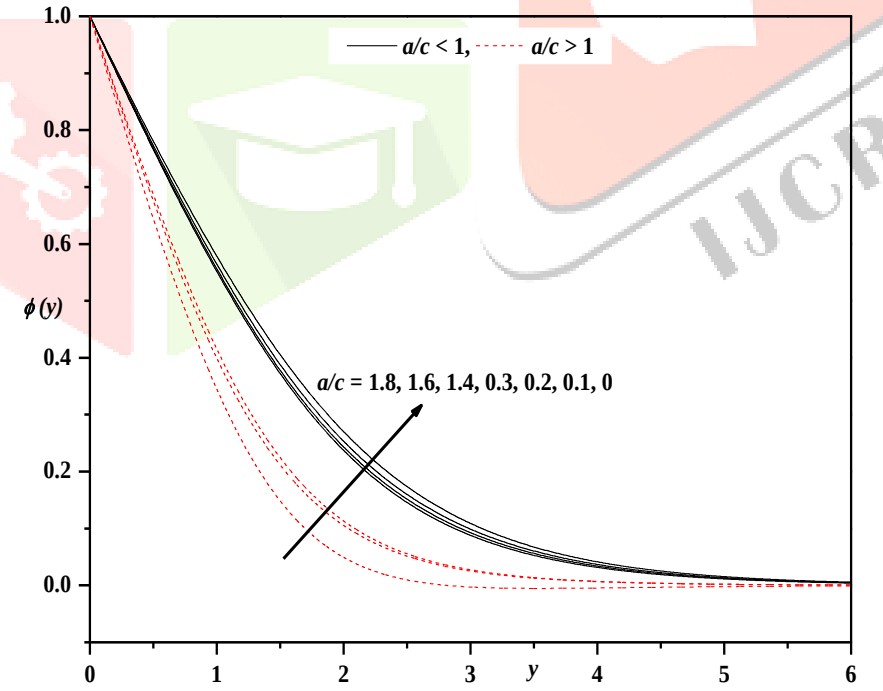

Fig.3(d):Concentration profile for different values of *a/c* with *Pr* = 1, *Sc* = 1, *Nt* = 0.1, *Nb* = 0.1, ε_1 = 0.1, ε_2 = 0.1, θ_r = -5, β = 2, γ = 0.5.

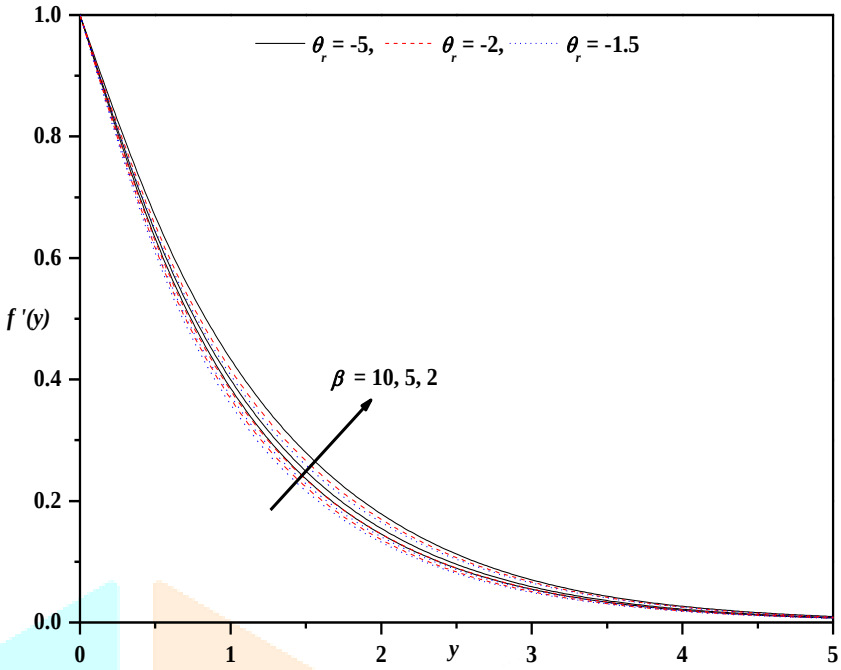

Fig.4(a):Axial velocity profile for different values of θ_r and β with Sc = 1, Nt = 0.1, Nb = 0.1, ε_1 = 0.1, Pr = 1, a/c = 0, ε_2 = 0.1, γ = 0.5.

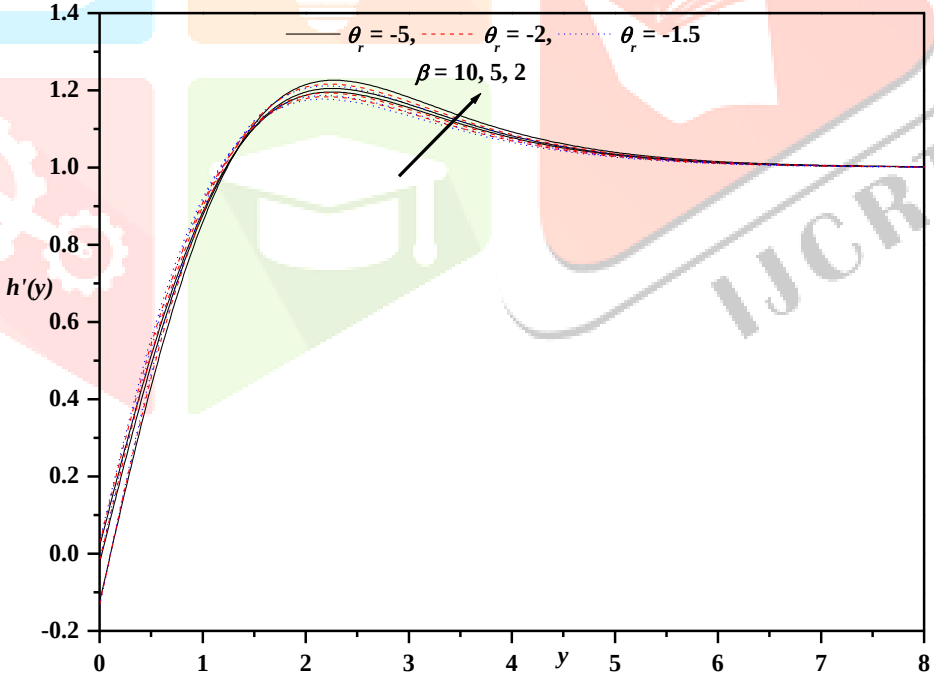

Fig.4(b):Transverse velocity profile for different values of θ_r and β with Sc = 1, Nt = 0.1, Nb = 0.1, ε_1 = 0.1, Pr = 1, a/c = 0.0, ε_2 = 0.1, γ = 0.5.

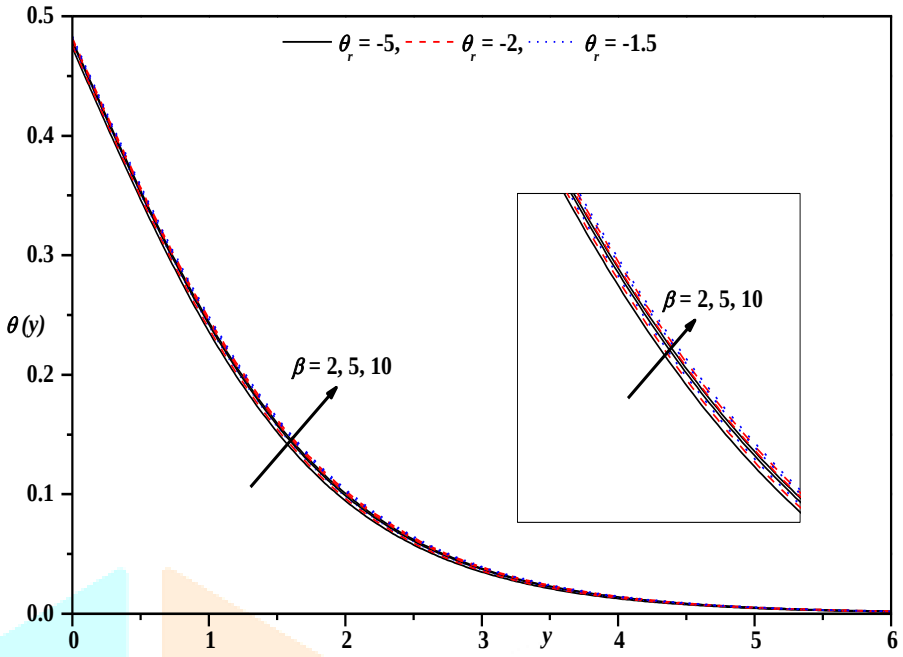

Fig.4(c):Temperature profile for different values of θ_r and β with Sc = 1, Nt = 0.1, Nb = 0.1, ε_1 = 0.1, Pr = 1, a/c = 0, ε_2 = 0.1, γ = 0.5.

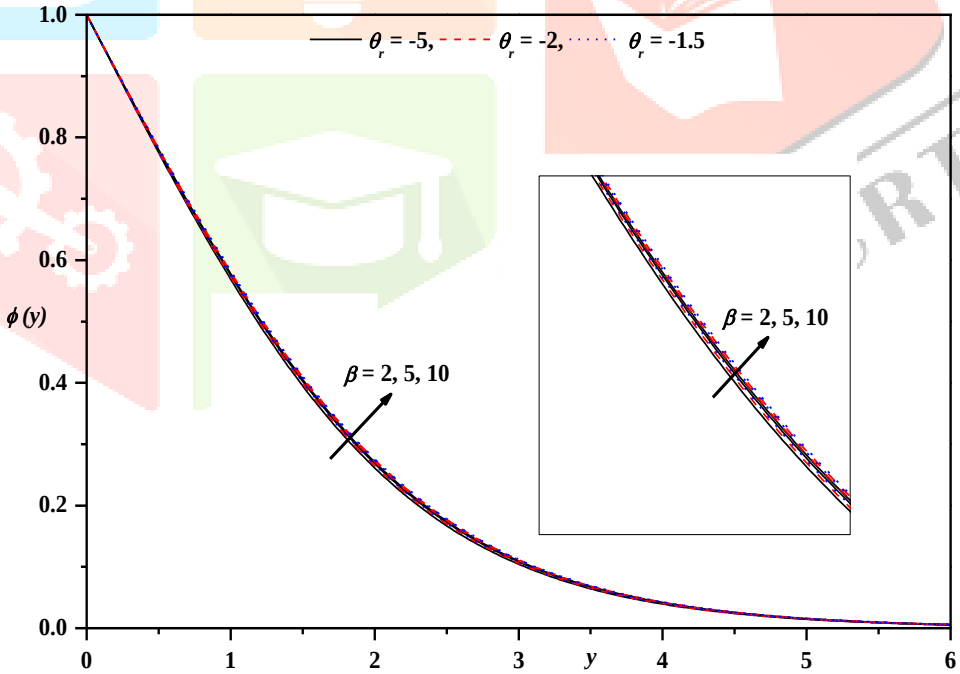

Fig.4(d):Concentration profile for different values of θ_r and β with Sc = 1, Nt = 0.1, Nb = 0.1, ε_1 = 0.1, Pr = 1, a/c = 0, ε_2 = 0.1, γ = 0.5.

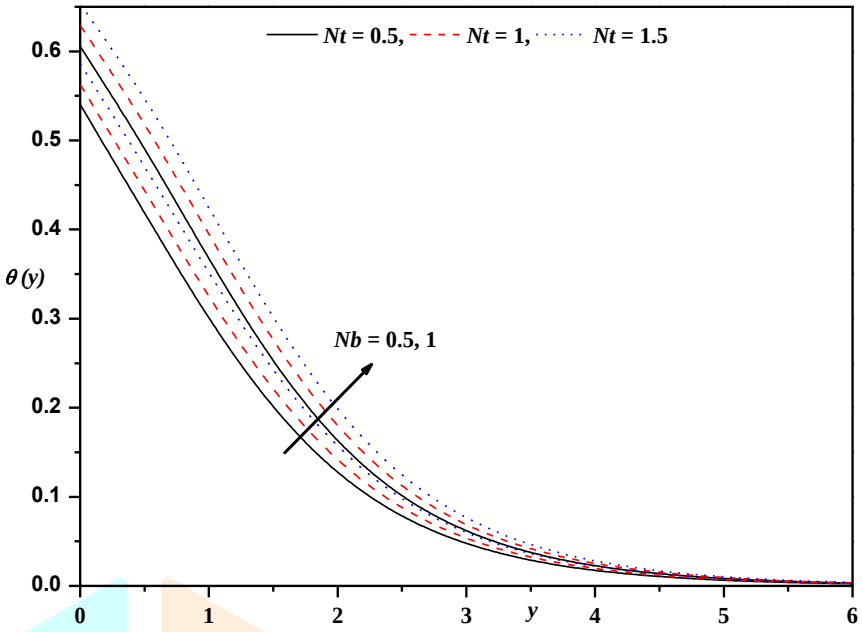

Fig.5(a):Temperature profile for different values of *Nt* and *Nb* with *Sc* = 1, ε_1 = 0.1, β = 2, θ_r = -5, *Pr* = 1, *a/c* = 0.01, ε_2 = 0.1, γ = 0.5.

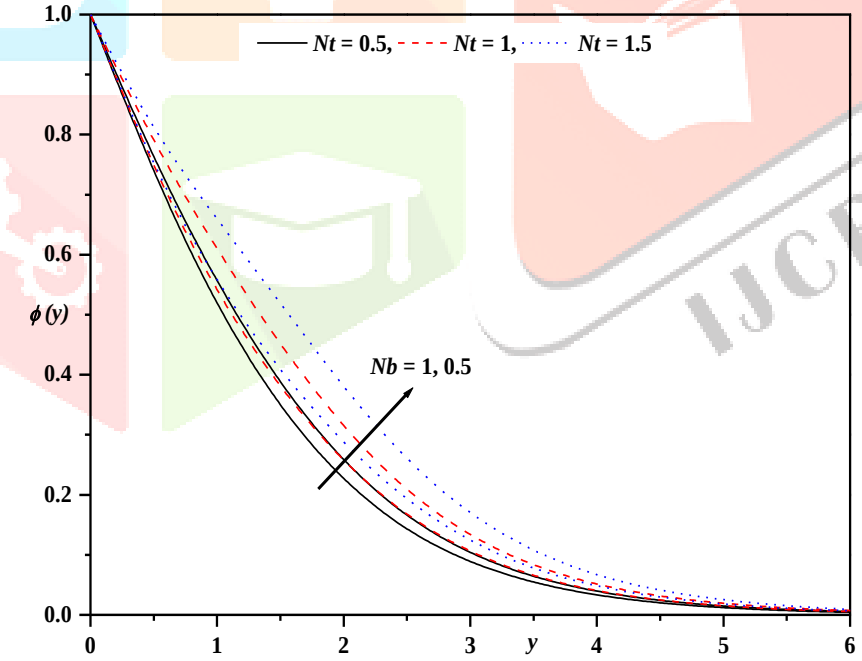

Fig.5(b):Concentration profile for different values of *Nt* and *Nb* with *Sc* = 1, ε_1 = 0.1, β = 2, θ_r = -5, *Pr* = 1, *a/c* = 0.01, ε_2 = 0.1, γ = 0.5.

Conclusion:

Analysis of oblique stagnation point flow of Casson nanofluid over a stretching sheet in the presence of variable fluid properties has been carried out. Obtained nonlinear partial differential equations (PDEs) are converted to dimensionless nonlinear ordinary differential equations (ODEs) via similarity transformations and are solved using Optimal Homotopy Analysis Method (OHAM). Following are some interesting conclusions:

- Axial velocity decreases with an increase in the variable viscosity parameter θ_r and the Casson parameter β whereas, it increases for increasing values of a/c . On the other hand, the dual effect of variable viscosity parameter θ_r and a/c is observed on transverse velocity.
- Thermal boundary layer thickness enhances for increasing values of variable viscosity parameter θ_r, Casson parameter β, thermal conductivity parameter ε_1, thermophoresis parameter Nt, Brownian motion parameter Nb and Biot number γ. On the contrary, the constant a/c and Prandtl number Pr decrease the thermal boundary layer thickness.
- Influence of variable viscosity parameter θ_r, Casson parameter β, thermophoresis parameter Nt and variable species diffusivity parameter ε_2 is to enhance the concentration boundary layer thickness and the reverse trend is observed for the constant a/c, the Brownian motion parameter Nb and the Schmidt number Sc.

References

[1]. K. Hiemenz, Die Grenzschicht an einem in den gleichformigen Flussigkeitsstrom eingetauchten geraden Kreiszylinder, Dinglers Polytech. J. 326 (1911) 321–324.

[2]. Y. Matunobu, Structure of pulsatile Hiemenz flow and temporal variation of wall shear stress near the stagnation point. I, J. Phys. Soc. Japan. 42 (1977) 2041–2049.

[3]. Y. Matunobu, Structure of pulsatile Hiemenz flow and temporal variation of wall shear stress near the stagnation point. II, J. Phys. Soc. Japan. 43 (1977) 326–329.

[4]. K. Tamada, Two-dimensional stagnation-point flow impinging obliquely on a plane wall, J. Phys. Soc. Japan. 46 (1979) 310–311.

[5]. H. Niimi, M. Minamiyama, S. Hanai, Steady axisymmetrical stagnation-point flow impinging obliquely on a wall, J. Phys. Soc. Japan. 50 (1981) 17–18.

[6]. T. Chiam, Stagnation-point flow towards a stretching plate, J. Phys. Soc. Japan. 63 (1994) 2443–2444.

[7]. T.R. Mahapatra, A.S. Gupta, Heat transfer in stagnation-point flow towards a stretching sheet, Heat

Mass Transf. 38 (2002) 517–521.

[8]. R. Nazar, N. Amin, D. Filip, I. Pop, Unsteady boundary layer flow in the region of the stagnation point on a stretching sheet, Int. J. Eng. Sci. 42 (2004) 1241–1253.

[9]. M. Reza, A.S. Gupta, Steady two-dimensional oblique stagnation-point flow towards a stretching surface, Fluid Dyn. Res. 37 (2005) 334.

[10]. Q. Wu, S. Weinbaum, Y. Andreopoulos, Stagnation-point flows in a porous medium, Chem. Eng. Sci. 60 (2005) 123–134.

[11]. F. Labropulu, D. Li, I. Pop, Non-orthogonal stagnation-point flow towards a stretching surface in a non-Newtonian fluid with heat transfer, Int. J. Therm. Sci. 49 (2010) 1042–1050.

[12]. O. D. Makinde, Heat and mass transfer by MHD mixed convection stagnation point flow toward a vertical plate embedded in a highly porous medium with radiation and internal heat generation. Meccanica, 47 (2012) 1173-1184.

[13]. O. D. Makinde, W. A. Khan, Z. H. Khan, Buoyancy effects on MHD stagnation point flow and heat transfer of a nanofluid past a convectively heated stretching/shrinking sheet. International Journal of Heat and Mass Transfer 62 (2013), 526-533.

[14]. W. A. Khan, O. D. Makinde, Z. H. Khan, Non-aligned MHD stagnation point flow of variable viscosity nanofluids past a stretching sheet with radiative heat. International Journal of Heat and Mass Transfer, 96 (2016) 525-534.

[15]. W. Ibrahim, O.D.Makinde, Magnetohydrodynamic stagnation point flow of a power-law nanofluid towards a convectively heated stretching sheet with slip. Proceedings of the Institution of Mechanical Engineers, Part E: Journal of Process Mechanical Engineering, 230(5), (2016), 345-354.

[16]. O.D. Makinde, W.A. Khan, Z.H. Khan, Stagnation point flow of MHD chemically reacting nanofluid over a stretching convective surface with slip and radiative heat. Proceedings of the Institution of Mechanical Engineers, Part E: Journal of Process Mechanical Engineering. 231(4) (2017) 695–703.

[17]. S. Nadeem, R. Mehmood, N.S. Akbar, Optimized analytical solution for oblique flow of a Casson-nano fluid with convective boundary conditions, Int. J. Therm. Sci. 78 (2014) 90–100.

[18]. A. Ishak, Similarity solutions for flow and heat transfer over a permeable surface with convective

boundary condition, Appl. Math. Comput. 217 (2010) 837–842.

[19]. P.O. Olanrewaju, O.T. Arulogun, K. Adebimpe, Internal heat generation effect on thermal boundary layer with a convective surface boundary condition, Am. J. Fluid Dyn. 2 (2012) 1–4.

[20]. S. Yao, T. Fang, Y. Zhong, Heat transfer of a generalized stretching/shrinking wall problem with convective boundary conditions, Commun. Nonlinear Sci. Numer. Simul. 16 (2011) 752–760.

[21]. A. Aziz, A similarity solution for laminar thermal boundary layer over a flat plate with a convective surface boundary condition, Commun. Nonlinear Sci. Numer. Simul. 14 (2009) 1064–1068.

[22]. A. Ghaffari, T. Javed, F. Labropulu, Oblique stagnation point flow of a non-Newtonian nanofluid over stretching surface with radiation: A numerical study, Therm. Sci. 21 (2017) 2139–2153.

[23]. K. V. Prasad, K. Vajravelu, H. Vaidya, M.M. Rashidi, Z.B. Neelufer, Flow and Heat Transfer of a Casson Liquid over a Vertical Stretching Surface: Optimal Solution, Am. J. Heat Mass Transf. 5 (2018) 1–22.

[24]. K. Vajravelu, K. V. Prasad, H. Vaidya, Influence of Hall Current on MHD Flow and Heat Transfer over a slender stretching sheet in the presence of variable fluid properties, Commun. Numer. Anal. 2016 (2016) 17–36.

[25]. K.V. Prasad, H. Vaidya, K. Vajravelu, P.S. Datti, V. Umesh, Axisymmetric mixed convective MHD flow over a slender cylinder in the presence of chemically reaction, Int. J. Appl. Mech. Eng. 21 (2016) 121–141.

[26]. K. V Prasad, H. Vaidya, K. Vajravelu, M.M. Rashidi, Effects of Variable Fluid Properties on MHD Flow and Heat Transfer over a Stretching Sheet with Variable Thickness, J. Mech. 33 (2017) 501–512.

[27]. K. V. Prasad, K. Vajravelu, H. Vaidya, B.T. Raju, Heat Transfer in a Non-Newtonian Nanofluid film Over a Stretching Surface, Journal of Nanofluids. 4 (2015) 536-547.

[28]. K. Vajravelu, K. V. Prasad, H. Vaidya, Influence of Hall Current on MHD flow and Heat transfer Over a Slender Stretching sheet in the Presence of Variable Fluid Properties, J. Communications in Numerical Analysis. 1 (2016) 17-36.

[29]. K.V. Prasad K. Vajravelu, I.S. Shivakumara, Hanumesh Vaidya and Neelufer .Z. Basha, Flow and Heat Transfer of a Casson Nanofluid Over a Nonlinear Stretching Sheet, Journal of nanofluids,

American Scientific Publishers, Vol. 5, 743-752 (2016).

[30]. K.V. Prasad, K. Vajravelu, H. Vaidya, Neelufer Z. Basha and V. Umesh, Thermal and species diffusion of MHD Casson fluid at a vertical sheet in the presence variable fluid properties, accepted for publication in Ain Sham Engineering Journal, Elsevier, http://dx.doi.org/10.1016/j.asej.2016.08.017.

[31]. S. Liao, An optimal homotopy-analysis approach for strongly nonlinear differential equations, Commun. Nonlinear Sci. Numer. Simul. 15 (2010) 2003–2016.

[32]. R.A. Van Gorder, Optimal homotopy analysis and control of error for implicitly defined fully nonlinear differential equations, Numer. Algorithms. (2018) 1–16. doi:10.1007/s11075-018-0540-0.